International Journal of Steel Structures 17(2): 535-541 (2017)
DOI 10.1007/s13296-017-6013-9
ISSN 1598-2351 (Print)
ISSN 2093-6311 (Online)

International Journal of
STEEL
STRUCTURES
www.springer.com/journal/13296

Strength of Double Skin Steel-Concrete Composite Walls

Ying Qin[1,2], Gan-Ping Shu[1,2], Sheng-Gang Fan[1,2], Jin-Yu Lu[1,2], Shi Cao[2], and Jian-Hong Han[2]

[1]*Key Lab of Concrete and Prestressed Concrete Structures of Ministry of Education, Southeast University, No. 2 Sipailou, Xuanwu District, Nanjing, Jiangsu, 210096, P.R. China*
[2]*School of Civil Engineering, Southeast University, No. 2 Sipailou, Xuanwu District, Nanjing, Jiangsu, 210096, P.R. China*

Abstract

Double skin steel-concrete composite walls have been increasingly used in civil engineering applications. However, the advantages of these walls have not been fully recognized due to the lack of appropriate technical guidelines for capacity design. In this paper, the local buckling strength of steel plate were firstly reviewed in terms of specifications incorporated in several modern codes. A methodology to predict the strength of steel plate with restraint of both concrete and shear studs was proposed based on the explicit solution for local buckling of steel plate in composite shear walls subjected to uniform axial compression and with elastically rotational restraint at loaded and unloaded edges. The results were compared with various previous experimental data and good agreement was observed. Furthermore, the load carrying capacity of composite walls was derived from the superposition of the contribution of steel plate and concrete. The predicted values from the proposed equations, together with the resulted determined from modern codes, were compared with the experimental results. It was found that both the proposed method and JEAG 4618 offer reasonable predictions while AISC 360 and KEPIC-SNG always underestimate the actual values.

Keywords: Composite shear wall, compression, local buckling, capacity design, modern codes

1. Introduction

Traditionally reinforced concrete structural walls has been widely-used in multi-story buildings to resist both gravity load and lateral load imposed by earthquake or wind (le Roux and Wium, 2012). Based on proper principle of capacity design, reinforced concrete walls can deform inelastically without significant loss of strength and stiffness. However, extensive research (Su and Wong, 2007) shows that the reinforced concrete walls exhibit poor ductility and deformation capacity when subjected to high axial load ratio. The upper limit for the axial load ratio is specified in modern codes and standards (EN 1998-1, 2008; ACI 318-08, 2008; GB 50011-2010, 2010). Eurocode 8 (EN 1998-1, 2008) requires that the axial load ratio should be no greater than 0.35 and 0.4 for reinforced walls with high and medium ductility, respectively. Chinese Code for seismic design of buildings (GB 50011-2010, 2010) limits the axial load ratio to be no greater than 0.5 for reinforced concrete walls in buildings higher than 80 m in severe seismic zones. Due to the requirements incorporated in these codes, the lower stories of high-rise buildings are often designed as rather thick sections. The ductility of reinforced concrete walls can also be achieved by arranging additional transverse reinforcement at the confined boundary elements. The lower bound of transverse reinforcement at the boundary elements of walls are also specified in modern codes to effectively confine the concrete in compression and prevent buckling of vertical rebars. This however, results in dense stirrups at the wall boundaries and causes construction difficulty (Qian *et al.*, 2012).

In recent years, a considerable amount of steel-concrete composite walls have been developed and applied to nuclear power plants and high-rise buildings in seismic regions. These walls, combining the best characteristics that steel and concrete have to offer, can be one of the alternatives for new forms of structural systems which have high strength and energy dissipation capacity under large axial compression and lateral load. As a matter of fact, steel-concrete composite structures have been widely used in engineering applications in the form of concrete-filled steel tubular columns (Mohanraj *et al.*, 2011). In general, steel-concrete composite walls can be classified into three categories. The first category is the steel-encased concrete composite walls, which have steel panel embedded in concrete walls. The second consists of a concrete core section integral with steel face plates,

Received June 29, 2016; accepted October 25, 2016;
published online June 30, 2017

*Corresponding author
E-mail: qinying@seu.edu.cn

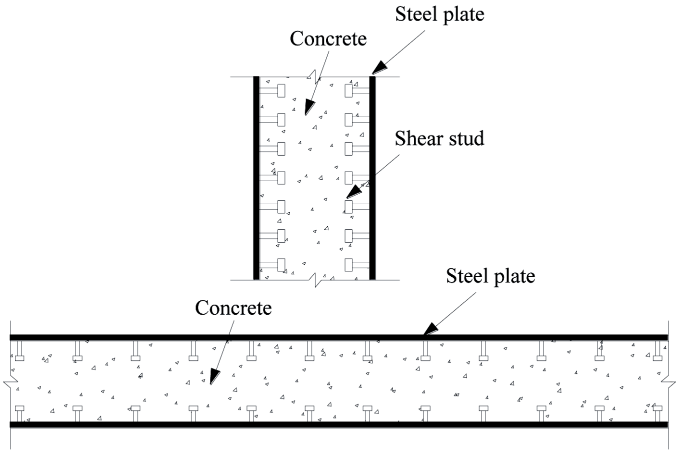

Figure 1. Typical double skin steel-concrete composite shear wall.

namely double skin composite walls. The third comprises steel or composite boundary frame and reinforced concrete infill wall.

A typical double skin composite wall normally contains no conventional in-plane reinforcement (i.e., vertical or horizontal rebar) or shear reinforcement (i.e., stirrups or T-headed bars). The steel skin plates are connected to the core concrete with regularly spaced shear studs or cross tie-bars as shown in Fig. 1. Double skin composite walls offer excellent architectural and structural merits over conventional reinforced concrete walls, particularly in terms of their strength-to-weight ratio, deformation capacity, and aesthetic appearance. Additionally, the steel skin plates can serve as a convenient formwork for pouring concrete and provide confinement for the cured concrete. By confining the concrete in a composite wall, an increase in the compressive strength of concrete will be achieved in addition to preventing the concrete from spalling while subjected to overload. Furthermore, the concrete inside the steel plate prevents the steel from buckling inwards. Despite the awareness of these advantages, this type of construction is still not being fully exploited due to the lack of guidelines in determining appropriately the design capacity. This dearth of information is even more pronounced with regards to the capacity of double skin composite walls subjected to axial compressive load.

Previous research on the experimental performance of double skin composite walls has included that of Eom *et al.* (2009), Ji *et al.* (2013), Nie *et al.* (2013), and Huang and Liew (2016). Eom *et al.* (2009) conducted cyclic tests to evaluate the seismic response of isolated and coupled double skin composite walls with rectangular and T-shaped cross sections. Ji *et al.* (2013) and Nie *et al.* (2013) proposed a new detailed composite wall and tested it under large axial compression and reversed cyclic lateral loading. The wall was composed of concrete filled tube columns at the boundaries and concrete filled double-steel-plate wall body that was either connected by tie bolts or divided into several compartments by vertical stiffeners transversely connected by distributed batten plates. Huang and Liew (2016) introduced J-hook connector to connect the external steel plates to improve the composite action between the steel face plates and concrete core to form an integral unit capable of resisting extreme loads. A series of tests were conducted to investigate the structural behavior of the proposed wall under combined compression and uniaxial bending.

Previous study on the analytical simulation of double skin composite walls has been conducted by Emori (2002), Hossain and Wright (2005), Vecchio and McQuade (2011), and Hu *et al.* (2014). Emori (2002) proposed the equations for ultimate compressive and shear strength based on superposition of the calculated strengths of steel plates and concrete. Hossain and Wright (2005) used a finite element model to simulate the axial load behavior of the composite wall consisting of double-skinned profiled steel sheet in filled with concrete. Vecchio and McQuade (2011) used the disturbed stress field model to analyze the wall elements. The computational model was incorporated into a two-dimensional nonlinear finite element analysis algorithm. Hu *et al.* (2014) developed an analysis program to investigate the moment-curvature behavior of composite walls based on a fiber section approach.

As can been seen from the literature review, few investigations considering the compressive capacity of composite walls have been conducted. Furthermore, the available equations specified in various design codes for general composite walls do not agree with each other as can be seen from the discussion in the following sections. Therefore, it is of importance to evaluate the accuracy of the prediction by modern codes. Meanwhile, there is a need to develop simply yet efficient approach to determine the strength of composite walls.

This paper first discussed the specifications related to the local buckling strength of steel plate incorporated in several modern design codes. Following an introduction of the explicit solutions by Qin (2016) for local buckling of steel plate in composite shear walls subjected to uniform axial compression and with elastically rotational restraint at loaded and unloaded edges, the equations to determine the local buckling strength of steel plate with shear studs inside was proposed. Based on the principle of superposition, the formula for the load carrying capacity of composite walls was developed. The presented analytical models were then compared with previous experimental data. The work in this paper provides design methodology for double skin steel-concrete composite walls applied in nuclear power plants. It can also be the basis for the development of design of double skin composite walls subjected to combined shear and compressive loadings in high-rise buildings.

2. Buckling of Steel Plate

2.1. Euler's column formula

The steel skin plate can be regarded as a column whose length and width correspond to the spaces between the shear studs along the vertical and horizontal direction, respectively. The surface plate buckles in between the shear stud rows. The buckling strength can then be derived from the Euler's column theory.

The critical load (or Euler load) $P_{cr,Euler}$ for columns under axial compressive load can be determined by

$$P_{cr,Euler} = \frac{\pi^2 EI}{(k_{Euler} l)^2} \tag{1}$$

where E is the elastic modulus of steel; I is the moment of inertia of plate; k_{Euler} is the effective length factor; and l is the equivalent length of the calculated plate and is equal to the space between the shear studs ($\overline{B}$).

Then the elastic buckling stress $\sigma_{cr,Euler}$ can be obtained by dividing the Euler load by the cross-sectional area of the steel plate as,

$$\sigma_{cr,Euler} = \frac{P_{cr,Euler}}{A} = \frac{\pi^2 E}{12k_{Euler}^2(\overline{B}/t)^2} \tag{2}$$

where A is the cross-sectional area of the steel skin plate; and t is the thickness of the steel skin plate.

2.2. American standard AISC 360-10

The critical stress, $\sigma_{cr,AISC}$, in Specification for Structural Steel Buildings ANSI/AISC 360-10 (2010) is specified in Section E3 and determined as follows:

(a) When $\frac{KL}{r} \le 4.71\sqrt{\frac{E}{F_y}}$ (or $\frac{F_y}{F_e} \le 2.25$)

$$\sigma_{cr,AISC} = \left(0.658^{\frac{F_y}{F_e}}\right) F_y \tag{3}$$

(b) When $\frac{KL}{r} > 4.71\sqrt{\frac{E}{F_y}}$ (or $\frac{F_y}{F_e} > 2.25$)

$$\sigma_{cr,AISC} = 0.877 F_e \tag{4}$$

where K is the effective length factor of members subjected to compression and shall be taken as 1.0 for composite walls; L is the laterally unbraced length of the wall; r is the radius of gyration; F_y is the specified minimum yield stress; and F_e is the elastic buckling stress determined by Eq. (5). Note that the two inequalities for calculating the limits, one based on $\frac{Kl}{r}$ and one based on $\frac{F_y}{F_e}$, provide the same result.

$$F_e = \frac{\pi^2 E}{\left(\frac{KL}{r}\right)^2} \tag{5}$$

2.3. Japanese standard JEAG 4618-2005

According to technical guidelines for seismic design of steel plate concrete structures JEAG 4618-2005 (2005), the buckling load ($P_{cr,JEAG}$) and the elastic buckling stress ($\sigma_{cr,JEAG}$) can be calculated as

$$P_{cr,JEAG} = \sigma_{cr,JEAG} A \tag{6}$$

(a) When $\frac{\overline{B}}{t} \le 600/\sqrt{f_y}$

$$\sigma_{cr,JEAG} = f_y \tag{7}$$

(b) When $\frac{\overline{B}}{t} > 600/\sqrt{f_y}$

$$\sigma_{cr,JEAG} = \frac{\pi^2 E}{12k_{JEAG}^2(\overline{B}/t)^2} \tag{8}$$

where f_y is the yield strength of the steel; k_{JEAG} is the effective length factor and can be taken as 0.7 and the other parameters have been previously defined.

2.4. South Korea standard KEPIC-SNG

Based on the South Korea design code KEPIC-SNG (KEA 2010), the compressive capacity of the steel skin plate ($P_{cr,KEPIC}$) can be determined as

$$P_{cr,KEPIC} = \sigma_{cr,KEPIC} A \tag{9}$$

The corresponding buckling stress is calculated by

$$\sigma_{cr,KEPIC} = \left(1.5 - 0.043\frac{k_{KEPIC}\overline{B}}{t} - 90\varepsilon_n\right) f_y < f_y \tag{10}$$

where k_{KEPIC} is the effective length and can be taken as 0.5, ε_n is the nominal compressive strain and can be taken as 0.002 and the other parameters have been previously defined.

2.5. Proposed equations

Qin (2016) proposed an explicit formulas for local buckling of steel plate in composite shear walls subjected to uniform axial compression and with elastically rotational restraint at loaded and unloaded edges. It is normally assumed that the steel plate is clamped at the loaded edges and simply supported at the unloaded edges. The corresponding critical local buckling stress $\sigma_{cr,c}$ is given by,

$$\sigma_{cr,c} = \frac{5.467\pi^2 E}{12(1-v^2)(B/t)^2} \tag{11}$$

where B is the width of steel plate in composite wall, v is the Poisson's ratio of steel and can be taken as 0.3 and the other parameters have been previously defined.

However, the presence of shear studs was not considered in the above solution. For the composite wall which has shear stud to enhance the composite action between the steel plate and infilled concrete, the shear studs do provide restraint to the steel plate. It may argue that the restraint offered by shear studs is not as strong as that by the adjacent plate. As a matter of fact, one half-wave was observed to develop across approximately two rows of shear studs (Chen *et al.*, 2015). Consequently, the width of steel plate (B) in Eq. (11) was replaced by two times the spacing between shear studs ($2\overline{B}$) to account for the effect of shear studs, as given by,

$$\sigma_{cr,p} = \frac{5.467\pi^2 E}{48(1-v^2)(\overline{B}/t)^2} \le f_y \tag{12}$$

The limits for stud spacing-to-plate thickness ratios ($\overline{B}/t$) can be determined from Eq. (12). The elastic modulus of steel was taken as $E = 2.06\times10^5$ MPa, and Possion's ratio $v = 0.3$.

$$(\overline{B}/t) = \sqrt{\frac{5.467\pi^2 E}{48 f_y (1-v^2)}} = \frac{504}{\sqrt{f_y}} \tag{13}$$

Therefore, the local buckling strength can be calculated as,

$$\sigma_{cr,p} = f_y \quad \text{if } \frac{\overline{B}}{t} \le \frac{504}{\sqrt{f_y}} \tag{14a}$$

$$\sigma_{cr,p} = \frac{5.467\pi^2 E}{48(1-v^2)(\overline{B}/t)^2} \quad \text{if } \frac{\overline{B}}{t} > \frac{504}{\sqrt{f_y}} \tag{14b}$$

2.6. Comparison with database

Researchers in Japan (Sakamoto *et al.*, 1985, Akiyama *et al.*, 1991, Usami *et al.*, 1995, Kanchi *et al.*, 1996) and South Korea (Choi and Han, 2009) have comprehensively investigated the compressive performance of composite walls by experiments. Thirty-five composite walls were tested with steel skin plates having stud spacing-to-plate thickness ratios ($\overline{B}/t$) ranging from 20 to 50. Zhang *et al.* (2014) once suggested to use the Euler's column buckling curve with effective length coefficient k_{Euler} equal to 0.7 to represent the critical buckling stress. However, it can be seen from Fig. 2 that Euler's column theory is the upper bound for the solution. It is on the unconservative side if Euler's formula is used to predict the critical buckling stress. The values calculated by the proposed equations were also plotted in Fig. 2. It can be found that, in general, the formulas proposed in the present study has better accuracy with the experimental values. It is also more conservative to employ Eq. (12) to approximate the potential critical local bucking strength of the composite walls.

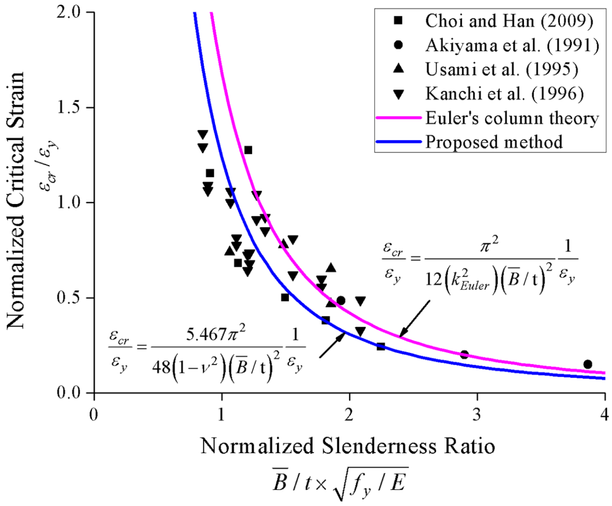

Figure 2. Comparison with previous data.

Zhang *et al.* (2016) tested four composite walls with double-skinned steel plate and infilled concrete subjected to concentric loadings with stud spacing-to-plate thickness ratios ranging from 20 to 56. The readers can refer to Zhang *et al.* (2016) for detailed information of the tests. The specimen details, along with the comparisons among the experimental data and estimated values from different modern codes and proposed formula in this paper, were provided in Table 1. It can be observed that both AISC 360 and KEPIC-SGN significantly underestimate the critical strains, while JEAG 4618 overestimate the experimental values. Relatively speaking, the proposed method in this paper provides the most suitable predictions for the tested data. Meanwhile, the impact of stud spacing-to-plate thickness ratio of the steel plate becomes significant for the cases where the local buckling occurs before the yielding.

Table 1. Comparison between the proposed values and the data by Zhang *et al.* (2016)

Specimen No.	Width×depth×thickness (mm×mm×mm)	$\overline{B}/t$	ε_e $\mu\varepsilon$	ε_{AISC} $\mu\varepsilon$	ε_{JEAG} $\mu\varepsilon$	ε_{KEPIC} $\mu\varepsilon$	$\varepsilon_{proposed}$ $\mu\varepsilon$
SCW-1	1160×1100×230	56	404	171	535	144	394
SCW-2	1160×1100×230	38	720	499	1162	625	855
SCW-3	1160×1100×230	31	981	677	1243	812	1243
SCW-4	1160×1100×230	20	N/A	965	1243	1106	1243

Note: ε_e is the measured critical strain from the tests; ε_{AISC}, ε_{JEAG}, ε_{KEPIC}, and $\varepsilon_{proposed}$ are the predicted values of strain by AISC 360, JEAG 4618, KEPIC-SGN, and the method proposed in this paper, respectively.

Table 2. Comparison for load carrying capacity of composite walls

Specimen No.	$\overline{B}/t$	N_e kN	N_{AISC} kN	N_{JEAG} kN	N_{KEPIC} kN	$N_{proposed}$ kN	N_e/N_{AISC}	N_e/N_{JEAG}	N_e/N_{KEPIC}	$N_e/N_{proposed}$
SCW-1	56	9380	8479	9185	8427	8912	1.11	1.02	1.11	1.05
SCW-2	38	12123	9115	10400	9359	9805	1.33	1.17	1.30	1.23
SCW-3	31	9976	9460	10557	9721	10557	1.05	0.94	1.03	0.94
SCW-4	20	11433	10018	10557	10291	10557	1.14	1.08	1.11	1.08
Average							1.16	1.05	1.14	1.08
Standard deviation							0.10	0.08	0.10	0.10

Note: N_e is the load carrying capacity recorded from the tests; N_{AISC}, N_{JEAG}, N_{KEPIC}, and $N_{proposed}$ are the predicted values of load carrying capacity by AISC 360, JEAG 4618, KEPIC-SGN, and the method proposed in this paper, respectively.

3. Strength of Composite Wall

3.1. Equation based on superposition

Having predicted the buckling strength of steel plate restrained by concrete, it is possible to determine the load carry capacity of composite wall (N_w) based on the summation of the contributions of the steel plate (N_s) and the infilled concrete (N_c), which assembles the method adopted by Choi *et al.* (2014), Hossain *et al.* (2015), and other researchers, as given by,

$$N_w = N_s + N_c \tag{15}$$

where N_s and N_c are calculated by the following equations,

$$N_s = \sigma_{cr,p} A_s \tag{16}$$

$$N_c = f_c A_c \tag{17}$$

where $\sigma_{cr,p}$ can be determined by Eqs. 14(a) and (b); A_s and A_c are the cross-sectional area of steel plate and concrete, respectively; f_c is the compressive strength of concrete and other parameters have been previously defined.

3.2. Validation of the proposed equations

In order to validate the accuracy of the proposed equations, the theoretical results from the formulas proposed above were compared to the data in the study conducted by Zhang *et al.* (2016). The predicted values by different modern codes were also provided. It should be noted that in Zhang *et al.*'s test, four plates were welded to form a box section and the concrete was poured inside. The local buckling would occur at the front and bottom plates rather than the side plates. Therefore, $\sigma_{cr,p}$ was used to obtain the contribution from the front and bottom plates while f_y was employed to calculate the contribution of the side plates.

Comparisons of the results among the previous experimental data (Zhang *et al.*, 2016), results from modern codes, and predicted values by the proposed equations are shown in Table 2. It can be found that among the four listed methods, in general, the load carrying capacity of composite walls can be appropriately estimated by the proposed method and JEAG 4618, while AISC 360 and KEPIC-SNG provide relatively conservative results for all specimens.

4. Conclusions

Analytical procedures for estimating the local buckling strength of steel plates and load carrying capacity of composite walls have been developed in this research. The following conclusions are based on the results and observations presented herein.

(1) The methods incorporated by several modern design codes were introduced. The proposed local buckling strength of steel plate with shear studs inside the wall was based on the classic plate analysis and the explicit solution for local buckling of steel plate in composite walls.

(2) The proposed method for load carrying capacity of composite walls rely on the superposition of the contributions from steel plate and concrete.

(3) The predicted results for local buckling of steel plate by the proposed methods agree best with the experimental results comparing to the prediction by other design codes. Meanwhile, the approximation for load carrying capacity of composite walls by both the proposed equation in this paper and JEAG 4618 provide reasonable values, while AISC 360 and KEPIC-SNG always overestimate the experimental data.

Acknowledgments

This work is sponsored by A Project Funded by the Priority Academic Program Development of Jiangsu Higher Education Institutions (PAPD) and Prospective Joint Research Project of Jiangsu Province, China (Grant No. BY2016076-06).

Notation

A	: cross-sectional area of the steel skin plate
A_s, A_c	: cross-sectional area of steel plate and concrete, respectively
B	: width of the plate in composite wall
$\overline{B}$	: space between the shear studs
E	: elastic modulus of steel
F_e	: elastic buckling stress
F_y	: specified minimum yield stress
f_c	: compressive strength of concrete
f_y	: yield strength of the steel
I	: moment of inertia of plate
K	: effective length factor of members subjected to compression
k_{Euler}	: effective length factor in Euler's column theory
k_{JEAG}	: effective length factor in JEAG-4618
k_{KEPIC}	: effective length factor in KEPIC-SNG
L	: laterally unbraced length of the wall
l	: equivalent length of the calculated plate
N_{AISC}	: predicted values of load carrying capacity by AISC 360
N_c	: contribution of concrete to load carry capacity of composite wall
N_e	: load carrying capacity recorded from the tests
N_{JEAG}	: predicted value of load carrying capacity by JEAG 4618
N_{KEPIC}	: predicted value of load carrying capacity by KEPIC-SGN
$N_{proposed}$	: predicted value of load carrying capacity by the proposed method
N_s	: contribution of steel plate to load carry capacity of composite wall
N_w	: load carry capacity of composite wall
$P_{cr,Euler}$	: Euler load
$P_{cr,JEAG}$	: buckling load by JEAG 4618
$P_{cr,KEPIC}$	: compressive capacity of the steel skin plate by KEPIC-SNG
r	: radius of gyration
t	: thickness of the steel skin plate
$\sigma_{cr,AISC}$	: critical stress specified in ANSI/AISC 360-10
$\sigma_{cr,c}$	: proposed critical local buckling stress
$\sigma_{cr,Euler}$	: critical buckling stress based on Euler's column theory
$\sigma_{cr,JEAG}$	: critical stress specified in JEAG 4618
$\sigma_{cr,KEPIC}$	: critical stress specified in KEPIC-SNG
$\sigma_{cr,p}$	: proposed critical local buckling stress
ε_{AISC}	: predicted values of strain by AISC 360
ε_e	: measured critical strain from the tests
ε_{JEAG}	: predicted values of strain by JEAG 4618
ε_{KEPIC}	: predicted values of strain by KEPIC-SGN
ε_n	: nominal compressive strain
$\varepsilon_{proposed}$	: predicted values of strain by the method proposed in this paper
v	: Poisson's ratio of steel

References

ACI 318-08 2008. Building code requirements for structural concrete and commentary. Farmington Hills: American Concrete Institute.

Akiyama, H., Sekimoto, H, et al (1991). "A compression and shear loading tests of concrete filled steel bearing wall." In: Transaction of 11th Structural Mechanics in Reactor Technology (SMiRT-11), pp. 323-328.

ANSI/AISC 360-10 (2010). Specification for Structural Steel Buildings. American Institute of Steel Construction, Chicago, Illinois.

Chen, L., Mahmoud, H., Tong, S., and Zhou, Y. (2015). "Seismic behavior of double steel plate–HSC composite walls." *Engineering Structures*, 102, pp. 1-12.

Choi, B.J., and Han, H.S. (2009). "An experiment on compressive profile of the unstiffened steel plate-concrete structures under compression loading." *Steel and Composite Structures*, 9(6), pp. 519-534.

Choi, B.J., Kang, C.K., and Park, H.Y. (2014). "Strength and behavior of steel plate–concrete wall structures using ordinary and eco-oriented cement concrete under axial compression." *Thin-Walled Structures*, 84, pp. 313-324.

Emori, K. (2002). "Compressive and shear strength of concrete filled steel box wall." *Steel Structures*, 2, pp. 29-40.

EN 1998-1 (2004). Eurocode 8: Design of structures for earthquake resistance-Part 1: general rules, seismic action and rules for buildings. CEN, Brussels: European Committee for Standardization.

Eom, T.S., Park, H.G., Lee, C.H., Kim, J.H., and Chang I.H. (2009). "Behavior of double skin composite wall subjected to in-plane cyclic loading." *Journal of Structural Engineering*, 135(10), pp. 1239-1249.

GB 50011-2010 (2010). Code for seismic design of buildings. Beijing: China Ministry of Construction.

Hossain, K.M.A., and Wright, H.D. (2005). "Finite element modelling of the shear behaviour of profiled composite walls incorporating steel-concrete interaction." *Structural Engineering and Mechanics*, 21(6), pp. 659-676.

Hossain, K.M.A., Mol, L.K., and Anwar, M.S. (2015). Axial load behaviour of pierced profiled composite walls with strength enhancement devices." *Journal of Constructional Steel Research*, 2015, pp. 48-64.

Hu, H.S., Nie, J.G., and Eatherton, M.R. (2014). "Deformation capacity of concrete-filled steel plate composite shear walls." *Journal of Constructional Steel Research*, 103, pp. 148-158.

Huang, Z., Liew, J.Y.R. (2016). "Structural behavior of steel–concrete–steel sandwich composite wall subjected to compression and end moment. *Thin-Walled Structures*, 98, pp. 592-606.

JEAG 4618-2005 (2005). Technical guidelines for seismic design of steel plate concrete structures: for buildings and structures. Architectural Institute of Japan.

Kanchi, M. et al (1996). Experimental study on a concrete filled steel structure Part 2 Compressive tests (1). In: Summary of Technical Papers of Annual Meeting, Architectural Institute of Japan, *Structures*, pp. 1071-1072.

Korea Electric Association (KEA) (2010). Steel-concrete structures (KEPIC-SNG), Korea Electric Power Industry Code.

le Roux, R.C., Wium, J.A. (2012). "Assessment of the behaviour factor for the seismic design of reinforced concrete structural walls according to SANS 10160-Part 4." *Journal of the South African Institution of Civil Engineering*, 54(1), pp. 69-80.

Miyauchi, Y. et al (1996). Experimental study on a concrete-filled steel structure, Part 3 Compressive test (2). *In: Summary of Technical Papers of Annual Meeting*, Architectural Institute of Japan, pp. 1073-1074.

Mohanraj, E.K., Kandasamy, S., and Malathy, R. (2011). "Behaviour of steel tubular stub and slender columns filled with concrete using recycled aggregates." *Journal of the South African Institution of Civil Engineering*, 53(2), pp. 31-38.

Ji, X., Jiang, F., and Qian, J. (2013). "Seismic behavior of steel tube-double steel plate-concrete composite walls: Experimental tests." *Journal of Constructional Steel Research*, 86, pp. 17-30.

Nie, J.G., Hu, H.S., Fan, J.S., Tao, M.X., Li, S.Y., and Liu, F.J. (2013). "Experimental study on seismic behavior of high-strength concrete filled double-steel-plate composite walls." *Journal of Constructional Steel Research*, 88, pp. 206-219.

Qian, J., Jiang, Z., and Ji, X. (2012). "Behavior of steel tube-reinforced concrete composite walls subjected to high axial force and cyclic loading." *Engineering Structures*, 36, pp. 173-184.

Qin, Y. (2016). "Local buckling of steel plate in double skin composite shear wall under axial compression." *Steel and Composite Structures*. (in review)

Sakamoto, M. et al (1985). Experimental study on concrete filled steel bearing wall Part 2: Compression characteristics. *In: Summary of Technical Papers of Annual Meeting*, Architectural Institute of Japan, Structures, pp. 1325-1326.

Su, R.K.L., and Wong, S.M. (2007). "Seismic behaviour of slender reinforced concrete shear walls under high axial load ratio." *Engineering Structures,* 29(8), pp. 1957-1965.

Usami, S., Akiyama, H., Narikawa, M., Hara, K., Takeuchi, M., and Sasaki, N. (1995). Study on a concrete filled steel structure for nuclear plants (part 2). Compressive loading tests on wall members. *In: Transaction of 13th Structural Mechanics in Reactor Technology (SMiRT-13)*, pp. 21-26.

Vecchio, F.J., and McQuade, I. (2011). "Towards improved modeling of steel-concrete composite wall elements." *Nuclear Engineering and Design*, 241(8), pp. 2629-2642.

Zhang, K., Varma, A.H., Malushte, S.R., and Gallocher, S. (2014). "Effect of shear connectors on local buckling and composite action in steel concrete composite walls." *Nuclear Engineering and Design*, 269, pp. 231-239.

Zhang, Y., Li, X., He, Q., and Yan, X. (2016). "Experimental study on local stability of composite walls with steel plates and filled concrete under concentric loads." *China Civil Engineering Journal*, 49(1), pp. 62-68.